DOE/ID-22183

MEASUREMENT OF SEDIMENTARY INTERBED HYDRAULIC PROPERTIES AND THEIR HYDROLOGIC INFLUENCE NEAR THE IDAHO NUCLEAR TECHNOLOGY AND ENGINEERING CENTER AT THE IDAHO NATIONAL ENGINEERING AND ENVIRONMENTAL LABORATORY

U.S. Geological Survey
Water-Resources Investigations Report 03-4048

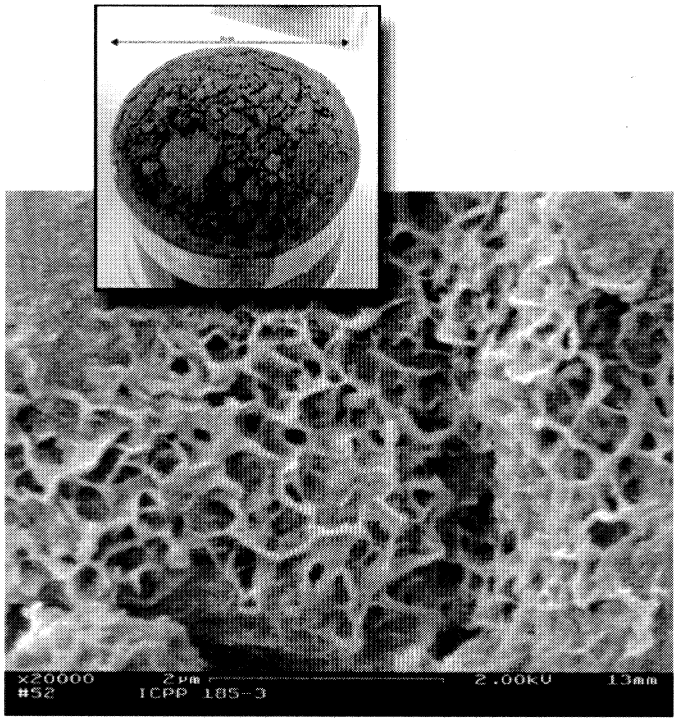

Upper interbed baked zone

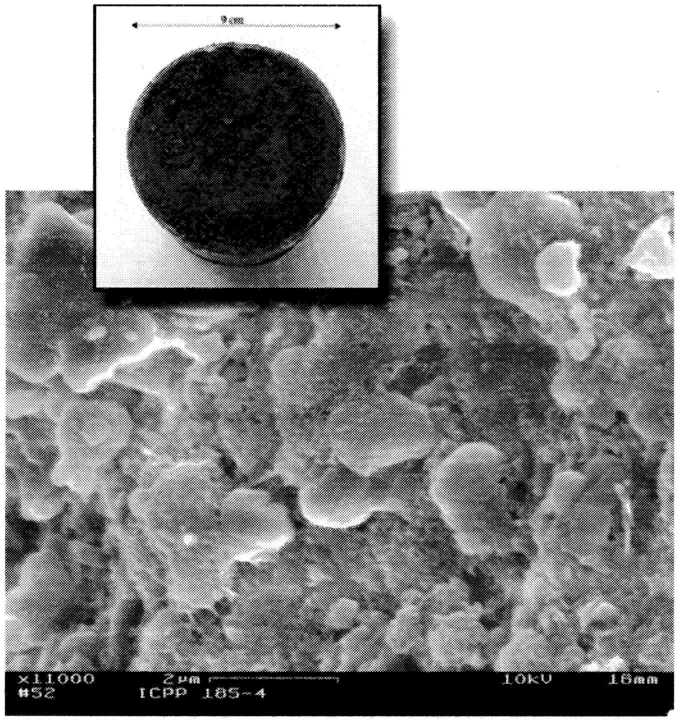

Lower interbed baked zone

Prepared in cooperation with the
U.S. DEPARTMENT OF ENERGY

USGS
science for a changing world

MEASUREMENT OF SEDIMENTARY INTERBED HYDRAULIC PROPERTIES AND THEIR HYDROLOGIC INFLUENCE NEAR THE IDAHO NUCLEAR TECHNOLOGY AND ENGINEERING CENTER AT THE IDAHO NATIONAL ENGINEERING AND ENVIRONMENTAL LABORATORY

By Kim S. Perkins

U.S. GEOLOGICAL SURVEY
Water-Resources Investigations Report 03-4048

Prepared in cooperation with the
U.S. DEPARTMENT OF ENERGY

Idaho Falls, Idaho
February 2003

U.S. DEPARTMENT OF THE INTERIOR
GALE NORTON, Secretary

U.S. GEOLOGICAL SURVEY
Charles G. Groat, Director

For additional information write to:

U.S. Geological Survey
INEEL, MS 1160
P.O. Box 2230
Idaho Falls, ID 83403

Copies of this report can be purchased from:

U.S. Geological Survey
Information Services
Box 25286, Federal Center
Denver, CO 80225

CONTENTS

FIGURES

TABLES

CONVERSION FACTORS

Multiply	By	To obtain
Centimeter (cm)	0.3937	Inch
Meter (m)	3.281	Foot
Square kilometer (km^2)	0.3861	Square mile
Cubic centimeter (cm^3)	0.06102	Cubic inch

Measurement of Sedimentary Interbed Hydraulic Properties and Their Hydrologic Influence Near the Idaho Nuclear Technology and Engineering Center at the Idaho National Engineering and Environmental Laboratory

by **Kim S. Perkins**

Abstract

Disposal of wastewater to unlined infiltration ponds near the Idaho Nuclear Technology and Engineering Center (INTEC), formerly known as the Idaho Chemical Processing Plant, at the Idaho National Engineering and Environmental Laboratory (INEEL) has resulted in the formation of perched water bodies in the unsaturated zone (Cecil and others, 1991). The unsaturated zone at the INEEL comprises numerous basalt flows interbedded with thinner layers of coarse- to fine-grained sediments and perched ground-water zones exist at various depths associated with massive basalts, basalt-flow contacts, sedimentary interbeds, and sediment-basalt contacts. Perched ground water is believed to result from large infiltration events such as seasonal flow in the Big Lost River and wastewater discharge to infiltration ponds. Evidence from a large-scale tracer experiment conducted in 1999 near the Radioactive Waste Management Complex (RWMC), approximately 13 km from the INTEC, indicates that rapid lateral flow of perched water in the unsaturated zone may be an important factor in contaminant transport at the INEEL (Nimmo and others, 2002b). Because sedimentary interbeds, and possibly baked-zone alterations at sediment-basalt contacts (Cecil and others, 1991) play an important role in the generation of perched water it is important to assess the hydraulic properties of these units.

In September 2001, the Vadose Zone Research Park (VZRP) was established near the INTEC for study of the movement of water and solutes through the unsaturated zone. Two new percolation ponds at the VZRP receive about a million gallons of equipment-cooling water each day. The subsurface at this location is much more complex than that near the RWMC and little is known about the hydraulic properties of the sedimentary interbeds. As part of an ongoing sedimentary interbed characterization project, hydraulic properties, including saturated and unsaturated hydraulic conductivity and water retention, were measured on 12 cores recovered from 2 interbeds from borehole ICPP-SCI-V-215 in the vicinity of the INTEC, which was drilled by the U.S. Geological Survey as a part of the development of the VZRP.

In general, the upper interbed examined in this study exhibits hydraulic properties consistent with higher clay contents than those of the lower interbed and also contains low permeability layers that could enhance perching. These interbeds, which are separated by a relatively thin basalt flow, also exhibit distinctly different baked-zone features that are apparent from visual and scanning electron microscope examination. Heat exposure from overlying lava flows produces baked zones at the tops of interbeds due to the dehydration and oxidation of iron-rich minerals. The baked zone of the upper interbed is macroporous, containing highly cemented aggregates, while the baked zone of the lower interbed contains highly oxidized, mainly unconsolidated sand. Baked-zone sediments from both interbeds, although texturally and structurally different, have comparable, relatively high saturated hydraulic conductivities.

In order to quantify the effect of the macroporous structure of the baked material in the upper interbed, water retention was measured on 2 undisturbed cores in addition to the 12 cores used for hydraulic property measurements. Water retention measurements were performed on the two undisturbed cores, then the cores were air dried, disaggregated, and repacked for additional

measurements in order to identify any structural effects.

INTRODUCTION

From 1952–84 low-level radioactive, chemical, and sanitary wastewater was disposed of from the Idaho Chemical Processing Plant (ICPP), now known as the Idaho Nuclear Technology and Engineering Center (INTEC) (fig. 1), directly to the Snake River Plain aquifer through a 183-m-deep disposal well. A wastewater infiltration pond was completed in February 1984 and used through 1985. A second pond was constructed in October 1985 and used through 1995. An average of 430 million gallons of wastewater per year (1963–93) was discharged to the deep disposal well and the unlined infiltration ponds, with an average annual discharge of 570 million gallons between 1992 and 1995 (Bartholomay and others, 1997). Chloride, fluoride, nitrate, sodium, and sulfate were the predominant chemicals discharged to the ponds between 1992 and 1995 and tritium accounted for more than 90 percent of the radioactivity in wastewater discharged at the ICPP since 1970. Other chemicals found in water samples include strontium-90, cesium-137, plutonium-239, plutonium-240, chromium, 1,1,1-trichloroethane, and various trace elements, such as aluminum, copper, iron, and manganese (Bartholomay, 1998). Perched ground-water zones have formed presumably as a result of the use of the unlined infiltration ponds to dispose of wastewater. Cecil and others (1991) identified perched water bodies at depths of 9.2 m where surficial sediments contact the uppermost basalt-flow group, at a 25.0 m contact of two basalt flows, at 54.3 m, possibly due to sedimentary fracture infilling, and at a 101.2 m-contact between two basalt flow units. Because of the complex nature of the subsurface near the INTEC, perching depths likely vary laterally.

A large-scale tracer experiment conducted in 1999 in the Big Lost River spreading areas (fig. 1) near the Radioactive Waste Management Complex (RWMC), approximately 13 km from the INTEC, showed that rapid lateral flow of perched water occurs in the unsaturated zone and may therefore be an important factor in contaminant transport (Nimmo and others, 2002b). In September 2001, a new field-scale research facility called the Vadose Zone Research Park (VZRP) was established in the vicinity of the INTEC (fig. 2). The park is a 2.6 km^2 facility for the study of the movement of water and solutes through unsaturated zone, which is about 150 m thick at this location. Two new percolation ponds were constructed to receive about a million gallons of equipment-cooling water each day.

Purpose and Scope

This report investigates the hydraulic characteristics of interbed material at one location near the INTEC and the possible effect of these characteristics on flow through the INEEL unsaturated zone. Saturated and unsaturated hydraulic properties were measured on minimally disturbed core samples recovered in the drilling of borehole ICPP-SCI-V-215 in June 2000 (fig. 2). These samples, except for the two additional samples that were repacked to examine structural effects on water retention, were carefully recored in the laboratory into the appropriate retainers for measurement of hydraulic conductivity (K) as a function of water content (θ) using the steady-state centrifuge (SSC) method (Nimmo and Mello, 1991; Conca and Wright, 1998). Hydraulic conductivity ($K(\theta)$) and matric potential (ψ) measurements were carried out on 12 samples from various depths in two interbeds located at depth intervals of 45.4 to 47.8 m and 58.2 to 60.4 m. An additional pair of cores from the upper interbed baked zone was used to examine structural effects on water retention.

Geohydrologic Setting

The eastern Snake River Plain is a structural basin about 325-km long and 80 to 110-km wide, bounded by mountain ranges and high plateaus. Streams within alluvial valleys separating the mountain ranges to the north and northwest flow onto the plain and the INEEL in response to rainfall and snowmelt. The eastern Snake River Plain is underlain by a sequence of basaltic lava flows interbedded with sedimentary deposits. The sediments consist of fluvial, lacustrine, and eolian deposits of clay, silt, sand, and gravel. Rhyolitic

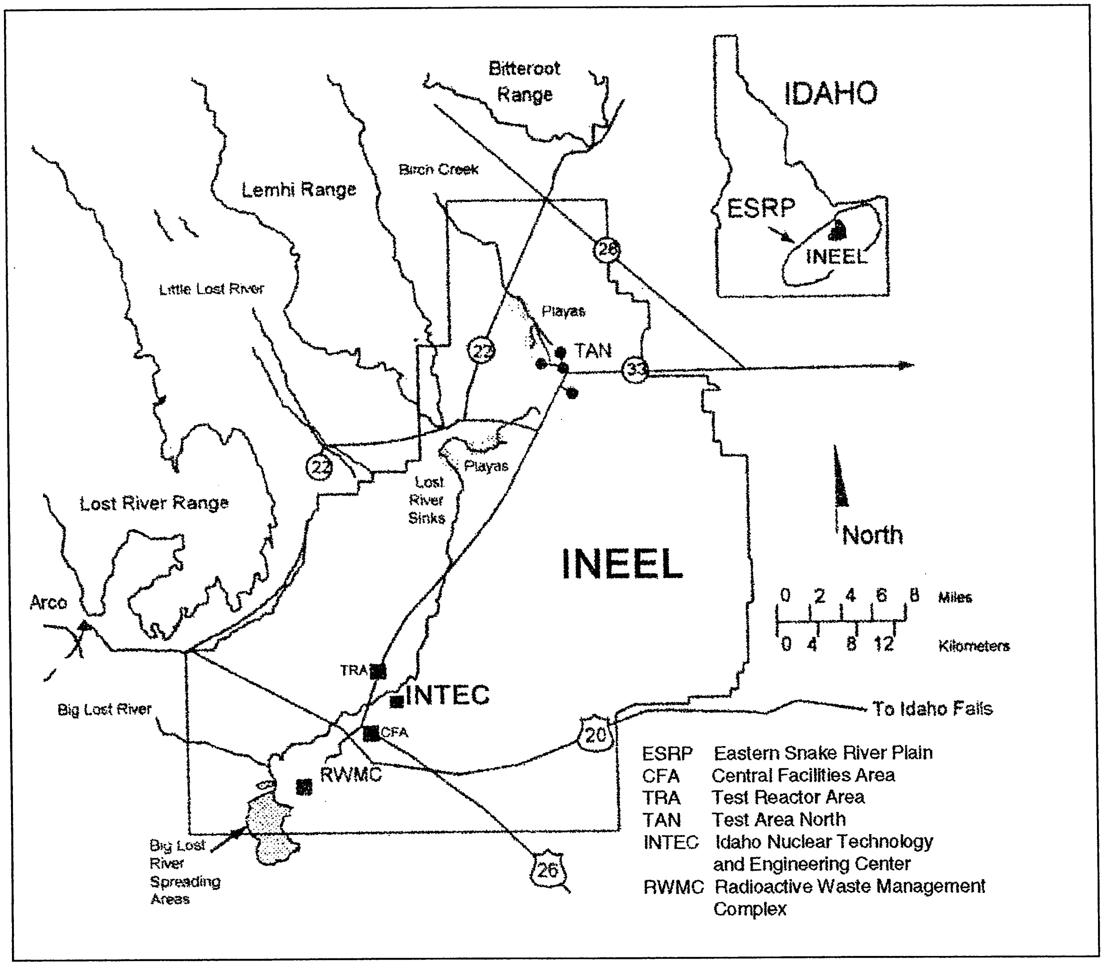

Figure 1. Map of the Idaho National Engineering and Environmental Laboratory (INEEL) including the Idaho Nuclear Technology and Engineering Center (INTEC), Radioactive Waste Management Complex (RWMC) and Big Lost River Spreading Areas.

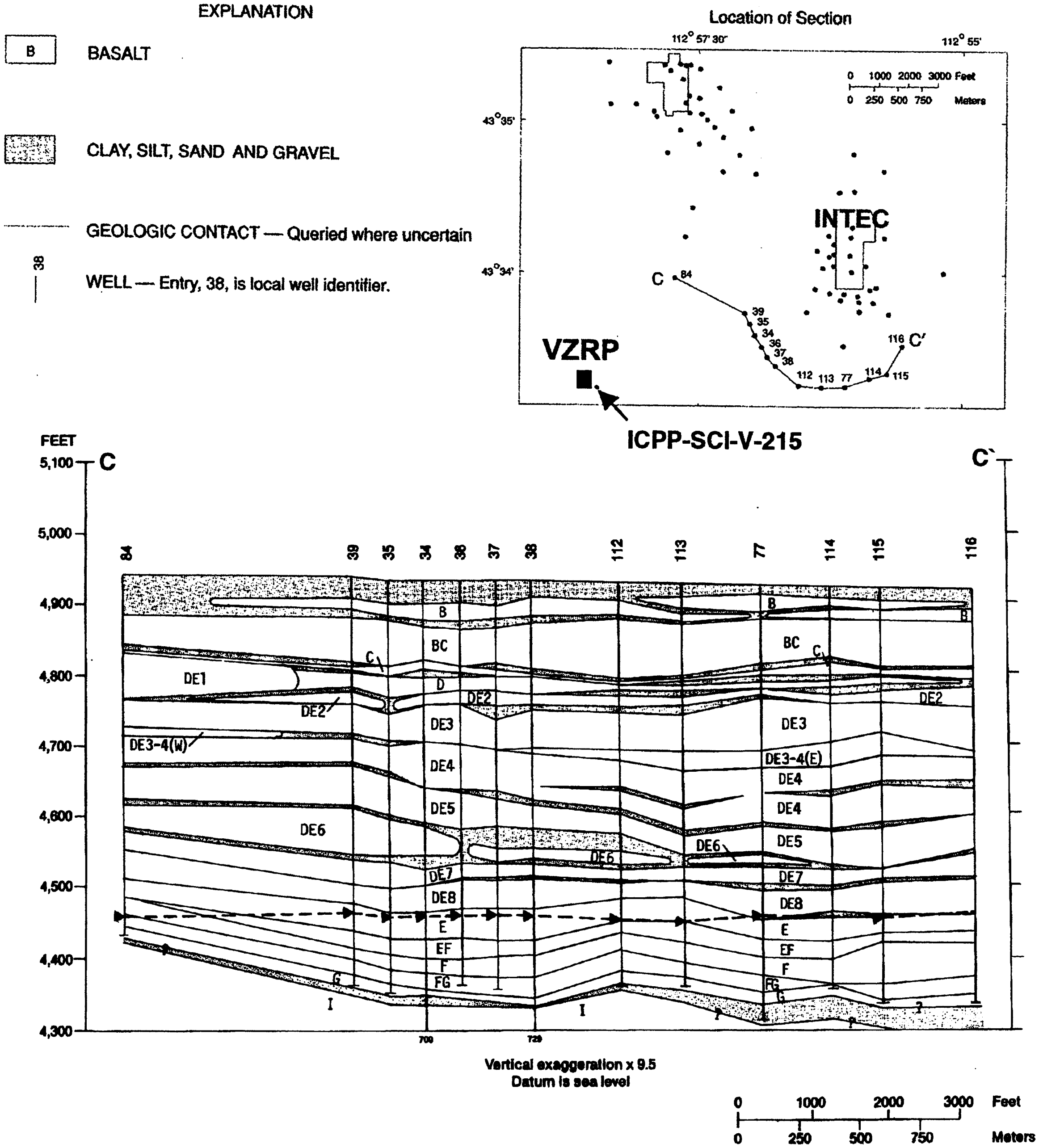

Figure 2. Subsurface cross section (C-C`) in the vicinity of the Idaho Nuclear Technology and Engineering Center (INTEC) (modified from Anderson, 1991). Locations of the Vadose Zone Research Park (VZRP) and borehole ICPP-SCI-V-215 are noted above.

lava flows and tuffs crop out locally at the surface and occur at depth below the basalt-sediment sequence (Mann, 1986). The INEEL occupies about 2,300 km^2 of semi-arid, sagebrush-covered terrain on the northwestern side of the plain. The INTEC is in the southern part of the INEEL covering approximately 0.4 km^2. The surficial sediments near the INTEC consist of gravelly material ranging from 0.6 to 22.2-m deep, being deepest to the west. In the vicinity of the INTEC, wells drilled to a depth of 213 m penetrate a sequence of 23 basalt flow groups and 15 to 20 sedimentary interbeds (Anderson, 1991, fig. 2).

METHODS

During the drilling of borehole ICPP-SCI-V-215, interbed sediment was cored into polycarbonate liners (roughly 8.6 cm inner diameter), capped off at the ends, and transported to the U.S. Geological Survey (USGS) Menlo Park Unsaturated Zone Flow Laboratory for analysis. The samples were cut into smaller recorable sections using a drill-type tool with a circular blade. Each section, unless there was obvious disturbance, was then recored using a mechanical recoring device. Liners were secured by clamps as the material was slowly extruded upward into a 5.2-cm long, 3.3-cm diameter retainer with a sharp-edged custom made stainless steel coring attachment. The retainers are designed specifically to fit into the buckets of the UFA[1]centrifugal rotor, which was used in the unsaturated hydraulic conductivity measurements described below (Nimmo and others, 2002a; Conca and Wright, 1998).

A Coulter LS-230 Particle Size Analyzer[1] was used to characterize particle-size distributions by optical diffraction (Gee and Or, 2002). The range of measurement for this particular device is 0.04–2,000 µm, which is divided into 116-size bins. Any particles above 2,000 µm were sieved out and later integrated into the size-distribution results. The fraction below 2,000 µm was carefully disaggregated using a mortar and rubber-tipped pestle, then split with a 16-compartment spinning riffler to obtain appropriate random samples for analysis. The material was sonicated for 60 seconds prior to each run and an average of 2 runs was calculated for each sample.

The standard falling head method for obtaining saturated hydraulic conductivity (K_{sat}) was used for most samples (Klute and Dirkson, 1986). For samples with low saturated conductivity, a modification of the standard method (Nimmo and Mello, 1991; Nimmo and others, 2002a) was performed in a centrifuge with saturated hydraulic conductivity calculated using the following equation:

$$K = [(-2la)/(A\rho\Delta tg)]\ln\left(\left(gz_f + \omega^2 r_b^2\right)/\left(gz_i + \omega^2 r_b^2\right)\right)$$

where

l = sample length (4.9 cm in this case),

a = the cross sectional area of the inflow reservoir (cm^2),

A = the cross sectional area of the sample (34.8 cm^2 in this case),

ρ = the density of the fluid used (1.0 g/cm^3 in this case),

t = time (seconds),

g = gravitational acceleration (9.8 cm/s^2),

z = the height of water in the reservoir (cm, initial-i, and final-f),

r = the radius of rotation at the sample bottom (13 cm in this case), and

ω = angular speed (rad/s).

The lab-saturated moisture content (table 1) was determined by weight at the end of the saturated conductivity measurement.

The SCC method used for obtaining unsaturated hydraulic conductivity is the UFA version (Conca and Wright, 1998; Nimmo and others, 2002a) of the method originally developed by Nimmo and others (1987). Steady-state, unsaturated flow through a core sample is achieved relatively quickly using centrifugal force to drive the liquid flow, with flux through the sample maintained precisely by a metering pump. A rotating seal assembly conducts the water from the pump to the spinning sample. The SSC method requires that steady-state conditions be established within a sample under centrifugal force. Steady-state conditions require a constant flow rate and a

---

[1] Use of brand names does not constitute endorsement by the U.S. Geological Survey

Table 1. Selected interbed properties for core samples from well ICPP–SCI–V–215 near the Vadose Zone Research Park at the Idaho National Engineering and Environmental Laboratory

Depth (m) U = upper interbed L = lower interbed	Calculated porosity (percent)	Lab saturated water content (cm^3/cm^3)	Saturated hydraulic conductivity (cm/s)	Texture (USDA)
45.85 U	0.5730	0.5773	2.17×10^{-04}	sandy loam
46.10 U	0.5530	0.4914	1.81×10^{-04}	sandy loam
46.37 U	0.4829	0.4733	4.68×10^{-05}	silt loam
46.45 U	0.4458	0.4516	1.68×10^{-05}	silt loam
47.12 U	0.4628	0.4786	2.22×10^{-07}	silt loam
47.42 U	0.4673	0.4961	1.66×10^{-07}	silt loam
58.36 L	0.5587	0.5542	3.36×10^{-04}	sand
58.55 L	0.5509	0.5681	1.42×10^{-03}	loamy sand
59.20 L	0.5075	0.5309	1.63×10^{-04}	sandy loam
59.48 L	0.4736	0.5182	4.34×10^{-04}	loamy sand
59.70 L	0.5403	0.5220	1.25×10^{-04}	sandy loam
59.92 L	0.4560	0.4856	3.95×10^{-04}	loamy sand

constant centrifugal force for sufficient time that both the water conditions and the water flux within the sample are constant. When these conditions are satisfied, Darcy's law relates K to θ and ψ for the established conditions. With centrifugal instead of gravitational force, Darcy's law takes the form

$$q = -K\,(d\psi/dr - \rho\omega^2 r)$$

where

q = the applied flow rate (cm/s),

r = the radius of centrifugal rotation (cm),

ρ = the density of the applied fluid (g/cm^3), and

ω = angular speed of rotation (rad/s).

If the driving force is applied with the centrifuge rotation speed large enough to ensure that $d\psi/dr << \rho\omega^2 r$ (i.e. any matric pressure gradients that develop in the sample during centrifugation are insignificant) the flow is essentially driven by centrifugal force alone. The flow equation then simplifies to

$$q = -K(\psi)\,\rho\omega^2 r.$$

The ω threshold for which the $d\psi/dr$ gradient can become negligible depends on the soil hydraulic properties. Nimmo and others (1987) discussed this gradient and presented model calculations showing that it becomes negligible at relatively low speeds for a sandy medium and at higher speeds for a fine-textured medium. This technique normally results in a fairly uniform water content throughout the sample, permitting the association of the sample average θ values with the measured ψ and K. After achieving steady flow within the centrifuge at a given q, the sample is removed, θ is determined by weight, and ψ is determined by a non-intrusive tensiometer or with the filter paper method (Campbell and Gee, 1986) in cases where suctions exceeded 800 cm. This method yields a triplet of data: K, θ, and ψ for the average moisture conditions within the sample. Repeat measurements with different q values (and perhaps different rotational speed) give the additional points needed to define the $K(\psi)$, $K(\theta)$, and $\psi(\theta)$ characteristic curves.

The SSC method as described above was used in this analysis with K, θ, and ψ measured in each run. There was no observable compaction of these samples due to centrifugal force, therefore the effect of such compaction on the hydraulic properties was assumed to be negligible.

Particle density measurements were performed with the pycnometer method (Blake and Hartge, 1986) on all samples. Porosity was calculated using the measured bulk- and particle-density values as described by Danielson and Sutherland (1986).

Because the upper and lower interbed baked zones were visually quite different, they were examined using a scanning electron microscope (LEO 982-Gemini column model, Schottky Field Emission-SEM[1]). Baked zone sediments from the upper interbed were highly aggregated, therefore water retention was also measured on two additional cores to examine structural effects using the controlled volume method (Winfield and Nimmo, 2002). With this method, water is incrementally extracted through a porous ceramic plate and pressure is measured with a tensiometer. Measurements were performed on the undisturbed samples which were then air dried, disaggregated with a mortar and rubber-tipped pestle, rewetted, and repacked to the original bulk density for additional measurements. The repacking technique consisted of adding sample to the retainer, wetting, tamping, and repeating until the desired bulk density was reached.

RESULTS AND DISCUSSION

The properties measured in this study include: bulk density, particle density, particle size distributions, soil moisture retention, saturated hydraulic conductivity, and hydraulic conductivity as a function of water content. Table 1 summarizes properties including calculated porosity, lab-saturated water content, saturated hydraulic conductivity, and U.S. Department of Agriculture texture classification (U.S. Department of Agriculture, 1951) for the 12 interbed core samples. In some cases, the lab-saturated water content is slightly higher than the calculated porosity value which may be due to the presence of excess water on top of the sample during weighing after the saturated hydraulic conductivity measurement. Unsaturated hydraulic conductivity and moisture retention data are presented in tabular form in table 2 and in graphical form in figures 3 and 4 respectively. The commonly used fitted parameters α and n were determined using the RETC program (van Genuchten and others, 1991) and are included in table 2. This program performs a non-linear least squares fit to the measured water retention and hydraulic conductivity data. The shape factors, α, an empirical parameter whose inverse is often referred to as the air entry value (van Genuchten, 1980), and n are required input for many models describing variably saturated flow.

Summarized particle-size distribution data are presented in tabular format in table 3 and graphical format in figure 5. In general, the upper interbed properties are consistent with a higher clay content than the lower interbed. Figure 6 shows the relationship between clay content and saturated hydraulic conductivity. In general, saturated hydraulic conductivity decreases as clay content increases. The water retention results from the two baked zone cores are discussed separately below.

This study provides vertical profiling of sedimentary interbed hydraulic properties at one location and two depth intervals. As earlier investigations also indicate, the sedimentary interbeds at the INEEL are highly complex with variable thickness, texture, and hydraulic properties. The variability of hydraulic properties in these samples, especially in the upper interbed, may be a major influence on perching at this location. Although the baked zones in these two interbeds are distinctly different with clay content having the greatest effect on unsaturated hydraulic properties, they are not likely to be a major influence on perching phenomena at this particular location. The layers below the baked zones where saturated hydraulic conductivity is low, for example at depths of 47.12 and 47.42 m, are more likely to influence perching.

Table 2. Hydraulic conductivity and water retention data for interbed core samples recovered from borehole ICPP-SCI-V-215 near the Vadose Zone Research Park at the Idaho National Engineering and Environmental Laboratory. ND means not determined and -0.01 cm matric potential is assumed at saturation

Depth (m), α and n parameters	Matric potential (cm water)	Volumetric water content (percent)	Hydraulic conductivity (cm/s)
45.85	-0.01	0.5773	2.173×10^{-04}
$\alpha = 1.1007$	-54.78	0.4623	1.637×10^{-05}
$n = 1.1296$	-73.40	0.4399	7.277×10^{-06}
	-102.57	0.4207	3.275×10^{-06}
	-118.11	0.4125	1.228×10^{-06}
	-135.78	0.4052	4.093×10^{-07}
	-201.19	0.3882	8.187×10^{-08}
	-311.83	0.3698	3.095×10^{-08}
	-409.10	0.3595	5.240×10^{-09}
46.10	-0.01	0.4914	1.810×10^{-04}
$\alpha = 0.3291$	-20.95	0.4346	1.637×10^{-05}
$n = 1.0602$	-37.76	0.4226	7.277×10^{-06}
	-50.72	0.4128	3.275×10^{-06}
	-59.04	0.4080	1.228×10^{-06}
	-149.81	0.3898	4.093×10^{-07}
	-157.59	0.3872	8.187×10^{-08}
	-224.20	0.3780	3.095×10^{-08}
	-424.49	0.3654	5.240×10^{-09}
46.37	-0.01	0.4733	4.675×10^{-05}
$\alpha = 0.0354$	-22.26	0.4542	1.637×10^{-05}
$n = 1.0067$	-38.36	0.4439	7.277×10^{-06}
	-64.83	0.4323	3.275×10^{-06}
	-86.83	0.4266	1.228×10^{-06}
	-159.31	0.4179	4.093×10^{-07}
	-361.26	0.4040	8.187×10^{-08}
	-594.66	0.3924	3.095×10^{-08}
	-1,620.17	0.3751	5.240×10^{-09}
	-9,642.34	0.3063	ND
46.45	-0.01	0.4516	1.678×10^{-05}
$\alpha = 0.0052$	-42.38	0.4453	1.637×10^{-05}
$n = 1.0886$	-46.02	0.4446	7.277×10^{-06}
	-62.69	0.4390	3.275×10^{-06}

Table 2. Hydraulic conductivity and water retention data for interbed core samples recovered from borehole ICPP-SCI-V-215 near the Vadose Zone Research Park at the Idaho National Engineering and Environmental Laboratory. ND means not determined and -0.01 cm matric potential is assumed at saturation--Continued

Depth (m), α and n parameters	Matric potential (cm water)	Volumetric water content (percent)	Hydraulic conductivity (cm/s)
	-96.97	0.4318	1.228×10^{-06}
	-292.92	0.4134	4.093×10^{-07}
	-587.97	0.4009	8.187×10^{-08}
	-871.32	0.3879	4.093×10^{-08}
	-2,451.24	0.3737	5.240×10^{-09}
	-17,067.67	0.2958	ND
47.12	-0.01	0.4786	2.217×10^{-07}
$\alpha = 0.0050$	ND	0.4172	1.048×10^{-07}
$n = 1.0849$	ND	0.4157	5.240×10^{-08}
	-945.91	0.4081	2.620×10^{-08}
	-1,088.55	0.4007	5.240×10^{-09}
	-1,654.32	0.3874	ND
	-8,962.61	0.3836	ND
47.42	-0.01	0.4964	1.660×10^{-07}
$\alpha = 0.0062$	ND	0.4505	1.067×10^{-07}
$n = 1.059$	ND	0.4415	5.335×10^{-08}
	-805.01	0.4417	2.668×10^{-08}
	-1,707.63	0.4381	5.335×10^{-09}
	-1,916.38	0.4267	ND
	-11,107.86	0.4235	ND
58.36	-0.01	0.5542	3.356×10^{-04}
$\alpha = 0.4077$	-69.50	0.2828	1.637×10^{-05}
$n = 1.2260$	-99.92	0.2407	7.277×10^{-06}
	-110.54	0.2301	3.275×10^{-06}
	-139.81	0.2137	1.228×10^{-06}
	-174.63	0.2020	4.093×10^{-07}
	-215.83	0.1921	8.187×10^{-08}
	-364.60	0.1741	3.095×10^{-08}
	-605.98	0.1582	5.240×10^{-09}
	-21,565.00	0.0888	ND
58.55	-0.01	0.5681	1.421×10^{-03}
$\alpha = 0.2830$	-105.72	0.3047	1.667×10^{-05}
$n = 1.2154$	-128.21	0.2717	7.410×10^{-06}

Table 2. Hydraulic conductivity and water retention data for interbed core samples recovered from borehole ICPP-SCI-V-215 near the Vadose Zone Research Park at the Idaho National Engineering and Environmental Laboratory. ND means not determined and -0.01 cm matric potential is assumed at saturation--Continued

Depth (m), α and n parameters	Matric potential (cm water)	Volumetric water content (percent)	Hydraulic conductivity (cm/s)
	-145.34	0.2560	3.335×10^{-06}
	-162.37	0.2433	1.250×10^{-06}
	-214.60	0.2238	4.168×10^{-07}
	-235.04	0.2152	8.336×10^{-08}
	-303.02	0.2006	3.152×10^{-08}
	-491.30	0.1816	5.335×10^{-09}
	-69,800.00	0.0954	ND
59.20	-0.01	0.5309	1.633×10^{-04}
$\alpha = 0.0065$	-131.57	0.4453	1.637×10^{-05}
$n = 1.4514$	-237.42	0.3881	7.277×10^{-06}
	-311.34	0.3498	3.275×10^{-06}
	-334.10	0.3377	1.228×10^{-06}
	-420.60	0.3132	4.093×10^{-07}
	-513.92	0.2913	8.187×10^{-08}
	-649.29	0.2703	3.095×10^{-08}
	-764.63	0.2544	5.240×10^{-09}
	-530.00	0.2520	ND
	-1,313.00	0.2485	ND
59.48	-0.01	0.5182	4.341×10^{-04}
$\alpha = 0.0204$	-114.95	0.2917	1.637×10^{-05}
$n = 1.6574$	-136.47	0.2459	7.277×10^{-06}
	-153.22	0.2226	3.275×10^{-06}
	-175.39	0.2010	1.228×10^{-06}
	-212.15	0.1830	4.093×10^{-07}
	-245.34	0.1707	8.187×10^{-08}
	-301.78	0.1611	3.095×10^{-08}
	-390.80	0.1438	5.240×10^{-09}
	-374.00	0.1407	ND
	-585.00	0.1373	ND
59.70	-0.01	0.5220	1.245×10^{-04}
$\alpha = 0.0124$	-35.21	0.4060	1.637×10^{-05}
$n = 1.3000$	-62.60	0.3898	7.277×10^{-06}
	-77.95	0.3830	3.275×10^{-06}

Table 2. Hydraulic conductivity and water retention data for interbed core samples recovered from borehole ICPP-SCI-V-215 near the Vadose Zone Research Park at the Idaho National Engineering and Environmental Laboratory. ND means not determined and -0.01 cm matric potential is assumed at saturation--Continued

Depth (m), α and n parameters	Matric potential (cm water)	Volumetric water content (percent)	Hydraulic conductivity (cm/s)
	-131.11	0.3748	1.228 x 10^{-06}
	-148.76	0.3731	4.093 x 10^{-07}
	-149.88	0.3715	8.187 x 10^{-08}
	-242.60	0.3632	3.095 x 10^{-08}
	-492.44	0.3520	5.240 x 10^{-09}
59.92	-0.01	0.4856	3.946 x 10^{-04}
$\alpha = 0.0347$	-71.21	0.3616	1.637 x 10^{-05}
$n = 1.3102$	-90.58	0.3231	7.277 x 10^{-06}
	-138.10	0.2801	3.275 x 10^{-06}
	-171.45	0.2631	1.228 x 10^{-06}
	-215.74	0.2501	4.093 x 10^{-07}
	-254.62	0.2399	8.187 x 10^{-08}
	-357.27	0.2251	3.095 x 10^{-08}
	-512.17	0.2100	5.240 x 10^{-09}

Table 3. Particle size distribution data summary (USDA Classification) for interbed core samples from borehole ICPP-SCI-V-215 near the Vadose Zone Research Park at the Idaho National Engineering and Environmental Laboratory

Depth (m)	Clay (<2 μm)	Silt (2–50 μm)	Very fine sand (50–100 μm)	Fine sand (100–250 μm)	Medium sand (250–500 μm)	Coarse sand (500–1000 μm)	Very coarse sand (1000–2000 μm)
45.85	4.6	25.0	7.7	16.3	22.1	21.0	3.3
46.10	4.5	20.8	5.0	11.9	16.1	27.8	14.0
46.37	13.5	64.5	10.9	14.7	0.1	0.0	0.0
46.45	9.1	50.4	8.7	19.4	7.6	3.3	1.5
47.12	15.2	73.0	9.6	2.3	0.0	0.0	0.0
47.42	15.0	66.1	10.3	8.6	0.1	0.0	0.0
58.36	1.4	7.7	9.4	32.2	35.8	12.9	0.6
58.55	2.0	16.8	17.4	43.0	16.9	3.8	0.1
59.20	4.1	43.4	22.8	20.7	3.8	4.3	0.9
59.48	1.9	13.4	28.6	55.0	1.2	0.0	0.0
59.70	6.5	20.5	4.8	13.9	19.0	19.7	15.6
59.92	4.3	19.0	15.9	35.8	20.6	4.4	0.0

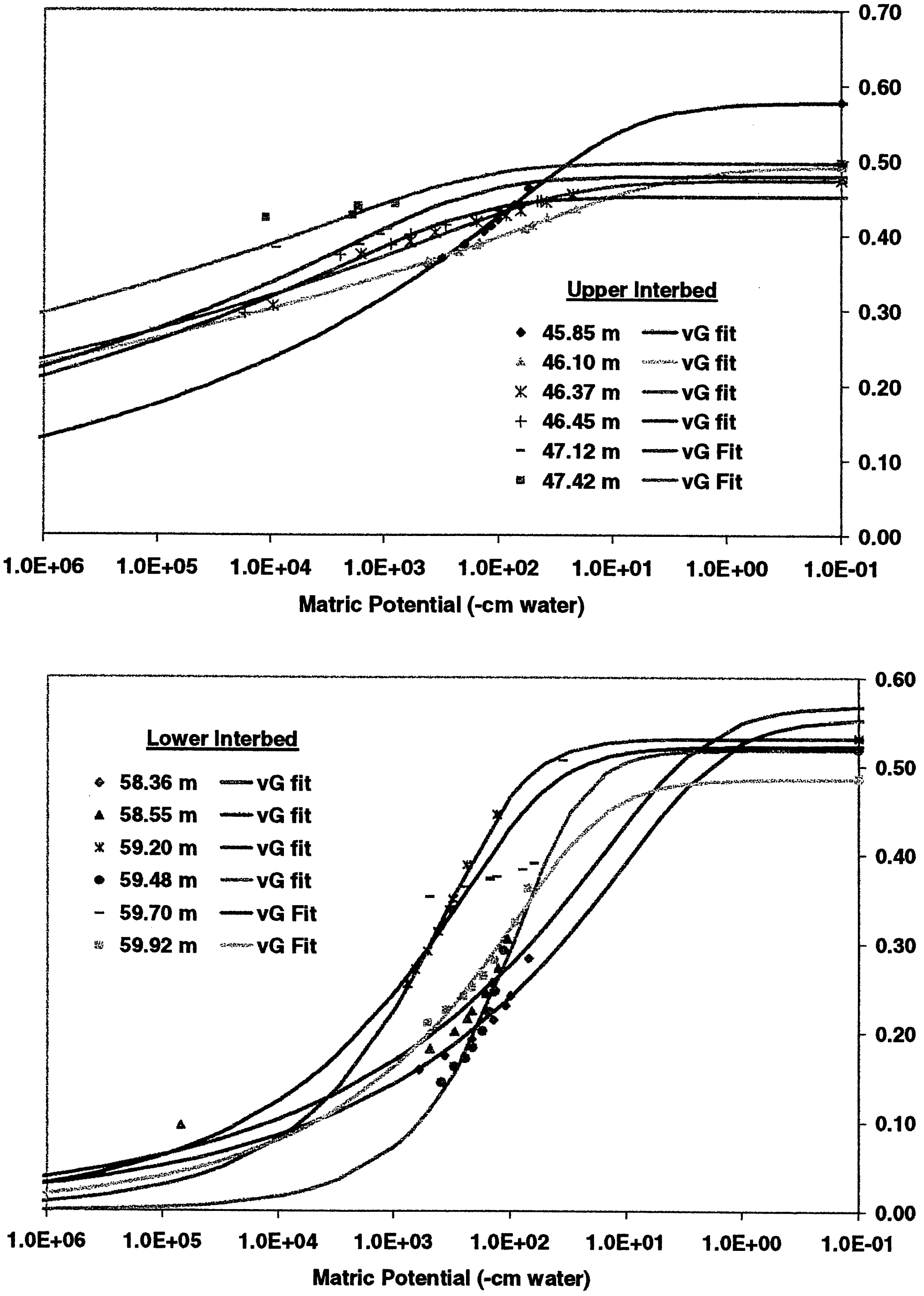

Figure 3. Water retention curves for the upper and lower interbeds from borehole ICPP-SCI-V-215 near the Vadose Zone Research Park (VZRP) at the Idaho National Engineering and Environmental Laboratory (INEEL). Data points were fit with the van Genuchten function (van Genuchten, 1980).

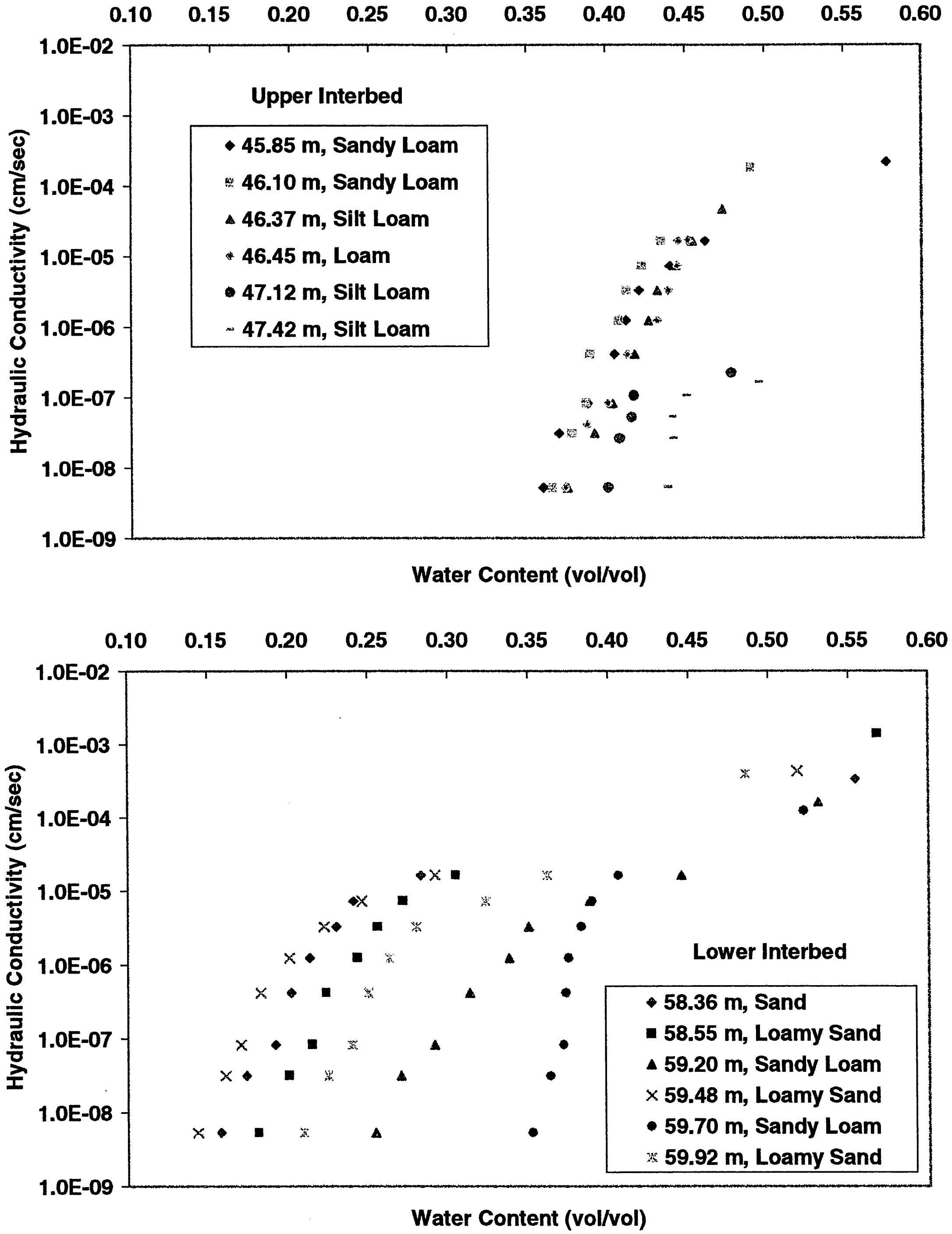

Figure 4. Unsaturated hydraulic conductivity data for the upper and lower interbeds from borehole ICPP-SCI-V-215 near the Vadose Zone Research Park (VZRP) at the Idaho National Engineering and Environmental Laboratory (INEEL).

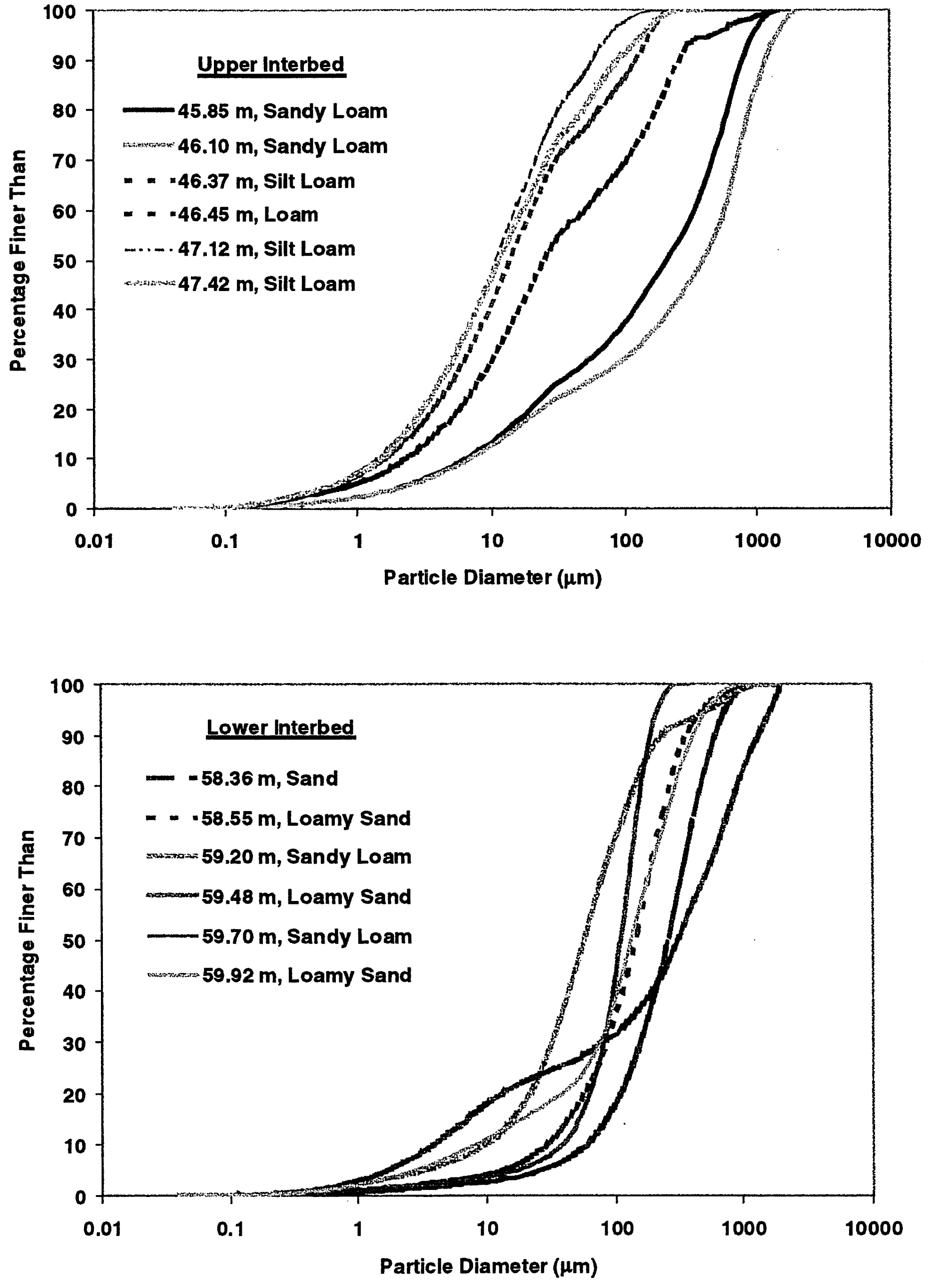

Figure 5. Cumulative particle size distributions for the upper and lower interbeds from borehole ICPP-SCI-V-215 near the Vadose Zone Research Park (VZRP) at the Idaho National Engineering and Environmental Laboratory (INEEL).

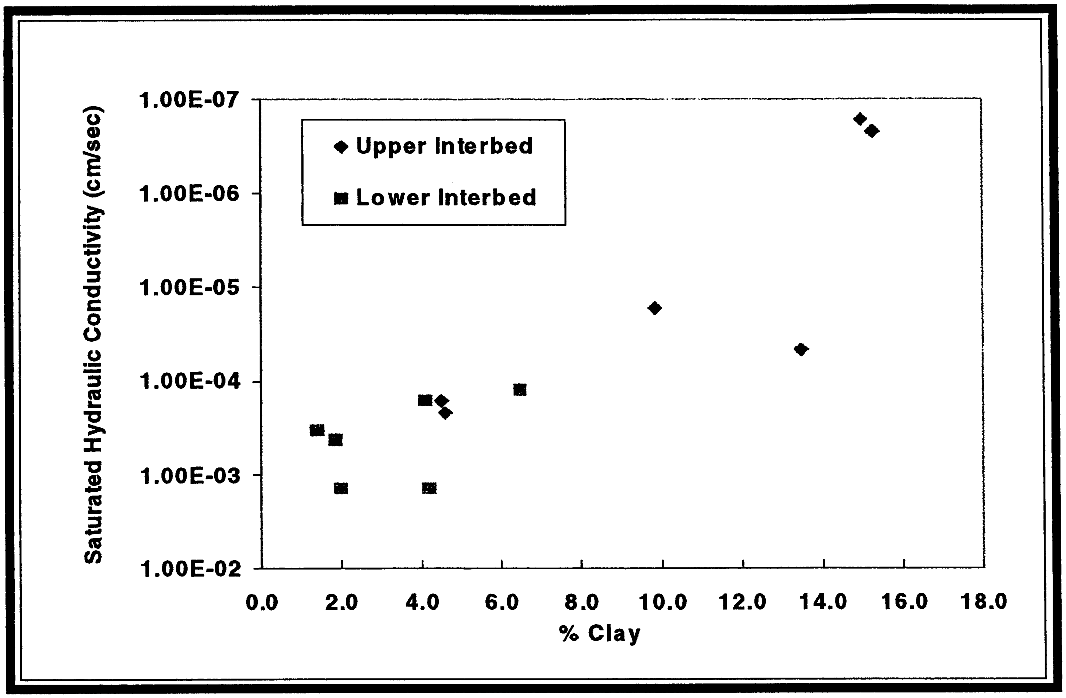

Figure 6. Clay content versus saturated hydraulic conductivity for the upper and lower interbeds from borehole ICPP-SCI-V-215 near the Vadose Zone Research Park (VZRP) at the Idaho National Engineering and Environmental Laboratory (INEEL).

REPACKING EXPERIMENT

In addition to the measurements reported above, two undisturbed cores from the highly aggregated baked zone sediments of the upper interbed were used to examine the effects of structure on water retention characteristics. In general, the upper interbed contains more fine material than the lower interbed, the effects of which are reflected in the hydraulic properties. The upper interbed baked zone is macroporous, containing highly cemented aggregates, while the baked zone of the lower interbed is highly oxidized and mainly unconsolidated. Scanning Electron Microscope (SEM) analysis shows distinct differences in the sediments from the two baked zones (fig. 7) and suggests that the cemented nature of the upper interbed may be due to clay coatings on grains that hardened during basalt deposition.

Controlled volume water retention measurements (Winfield and Nimmo, 2002) were performed on the two undisturbed cores from the upper baked zone. These were subsequently disaggregated and repacked; then the retention measurements were repeated. Results show the effect of the disruption of the macroporous structure on water retention (fig. 8). The retention curves are shifted to a more negative matric potential for a given water content in the wet range, indicating an overall decrease in average pore size. Pore size distributions were calculated based on capillary theory which relates the water retention function to the pore size distribution of the media; pores of different sizes drain at different pressures (Danielson and Sutherland 1986). The calculated distributions indicate a decrease in the mean pore size and a narrower range of sizes in the repacked samples (fig. 8). The creation of a more uniform pore size distribution as a result of the destruction of the largest and

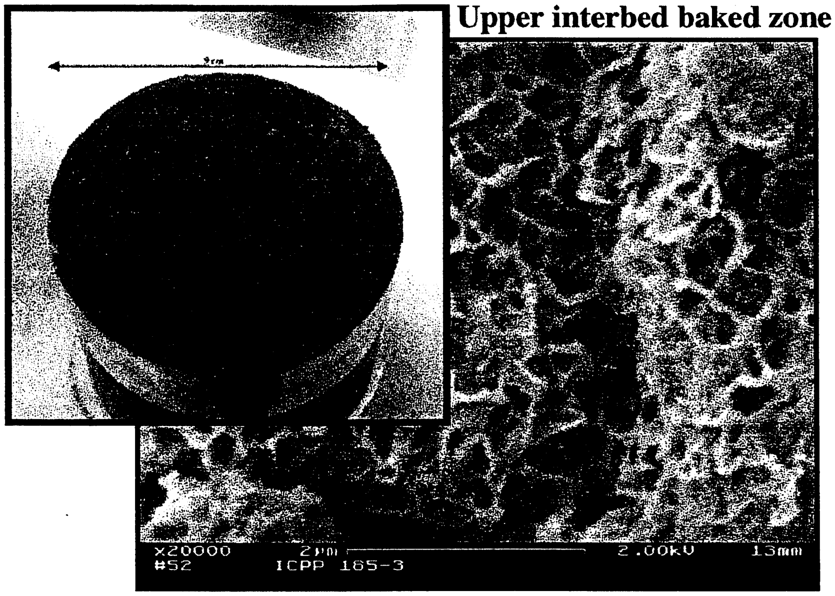

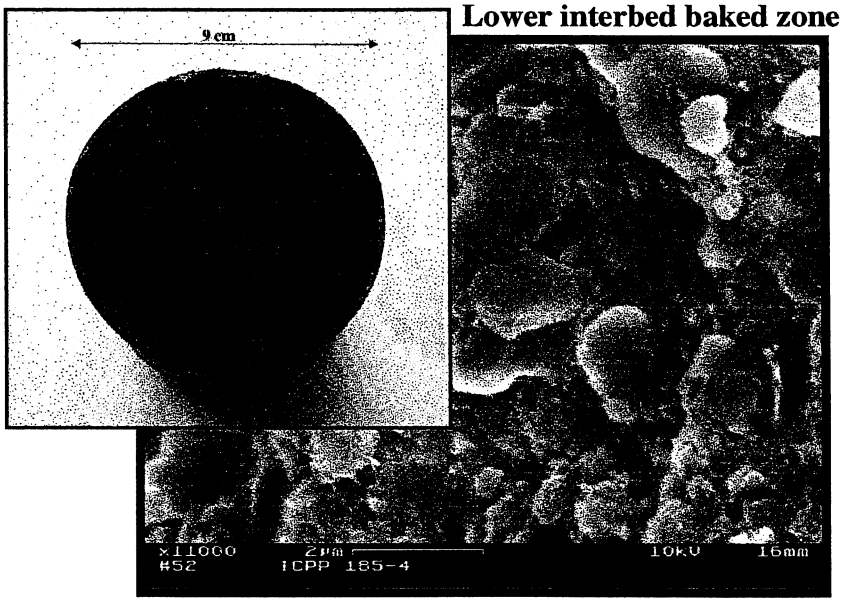

Figure 7. Core photographs and scanning electron microscope images for samples from the upper and lower interbed baked zones from borehole ICPP-SCI-V-215 near the Vadose Zone Research Park (VZRP) at the Idaho National Engineering and Environmental Laboratory (INEEL).

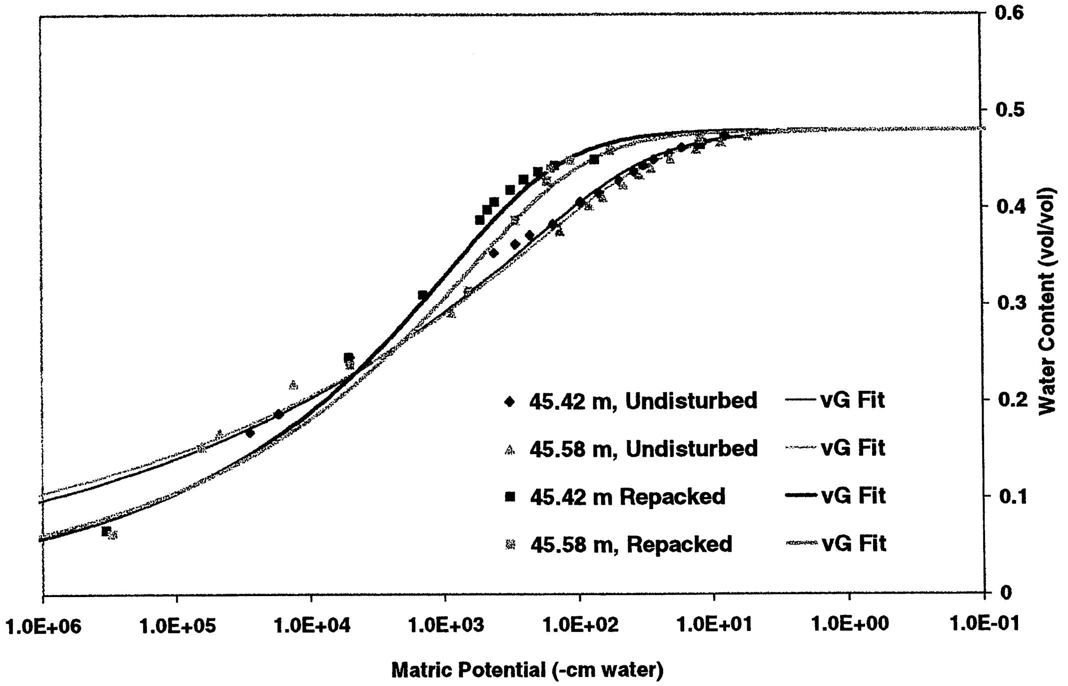

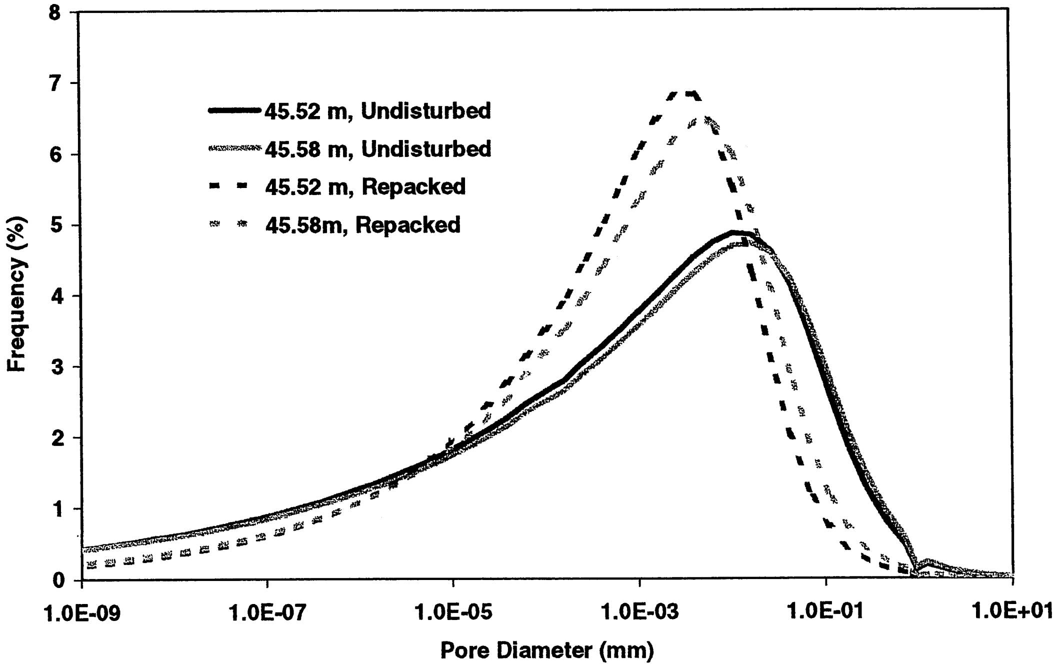

Figure 8. Water retention data (above) fit with the van Genuchten function (van Genuchten, 1980) and pore size distributions (below) calculated from the water retention data.

smallest pores would be expected to result in a steepening of the drainage retention curve (i.e. many pores of comparable size draining at about the same time), which is indeed the case.

CONCLUSIONS

The two interbeds at the location of ICPP-SCI-V-215, approximately 3 km southwest of the INTEC, have saturated hydraulic conductivity values that range over four orders of magnitude from 1.42 x 10^{-03} cm/s for loamy sand to 1.66 x 10^{-07} cm/s for silt loam. During high infiltration that occurs episodically from the Big Lost River and due to the disposal of wastewater to infiltration ponds, these interbeds, especially the upper interbed, may cause perching that leads to lateral flow through more permeable layers and overlying basalts. The baked zones in these interbeds are probably not the main influence on perching at this location.

The results presented here are consistent with those of past studies in showing a high degree of heterogeneity in the interbeds and, therefore, the need for analysis of a large number of samples from various locations and interbeds. Once further measurements are completed and the interbeds are better characterized, correlations between hydraulic properties and particle size distributions may permit the subsurface hydrology of other areas of the INEEL to be more easily assessed.

REFERENCES

Anderson, S.R., 1991, Stratigraphy of the unsaturated zone and uppermost part of the Snake River Plain aquifer at the Idaho Chemical Processing Plant and Test Reactors Area, Idaho National Engineering Laboratory, Idaho: U. S. Geological Survey Water-Resources Investigations Report 91–4010, 71 p.

Bartholomay, R.C., Tucker, B.J., Ackerman, D.J., and Liszewski, M.J., 1997, Hydrologic conditions and distribution of selected radiochemical and chemical constituents in water, Snake River Plain Aquifer, Idaho National Engineering Laboratory, Idaho, 1992 through 1995: U. S. Geological Survey Water-Resources Investigations Report 97–4086, 57 p.

Bartholomay, R.C., 1998, Distribution of selected radiochemical and chemical constituents in perched groundwater, Idaho National Engineering Laboratory, Idaho, 1992 through 1995: U. S. Geological Survey Water-Resources Investigations Report 98–4026, 59 p.

Blake, G.R., and Hartge, K.H., 1986, Particle Density: *in* A. Klute, ed., Methods of Soil Analysis, Part 1, American Society of Agronomy, Soil Science Society of America, Madison, Wisc., p. 377–382.

Campbell, G.S., and Gee, G W., 1986, Water Potential: Miscellaneous Methods: *in* A. Klute, ed., Methods of Soil Analysis, Part 1, American Society of Agronomy, Soil Science Society of America, Madison, Wisc., p. 628–630.

Cecil, L.D., Orr, B.R., Norton, T., and Anderson,S.R., 1991, Formation of perched ground-water zones and concentrations of selected chemical constituents in water, Idaho National Engineering Laboratory, Idaho, 1986–88: U. S. Geological Survey Water-Resources Investigations Report 91–4166, 53 p.

Conca, J.L., and Wright, J.V., 1998, The UFA method for rapid, direct measurement of unsaturated transport properties in soil, sediment, and rock: Australian Journal of Soil Research, v. 36, p. 291–315.

Danielson, R.E., and Sutherland P.L., 1986, Porosity: *in* A. Klute, ed., Methods of Soil Analysis, Part 1, American Society of Agronomy, Soil Science Society of America, Madison, Wisc., p. 444–445.

Gee, G.W., and Or, D., 2002, Particle-size analysis, *in* Dane, J.H., and Topp, G.C., eds., Methods of soil analysis, Part 4: Physical methods, American Society of Agronomy, Soil Science Society of America, Madison, Wisc., p. 255–293.

Klute, A., and Dirkson, C, 1986, Hydraulic conductivity and diffusivity: laboratory methods: *in* A. Klute, ed., Methods of Soil Analysis, Part 1, American Society of Agronomy, Soil Science Society of America, Madison, Wisc., p.687–734.

Mann, L.J., 1986, Hydraulic properties of rock units and chemical quality of water for INEL-1— a 10,365-foot deep test hole drilled at the Idaho National Engineering Laboratory, Idaho: U.S. Geological Survey Water-Resources Investigations Report 86-4020 (IDO–22070), 23 p.

Nimmo, J.R., Perkins, K.S., and Lewis, A.M., 2002a, Steady-state centrifuge: *in* Dane, J.H., and Topp, G.C., eds., Methods of soil analysis, Part 4: Physical methods, American Society of Agronomy, Soil Science Society of America, Madison, Wisc., p. 903–916.

Nimmo, J.R., Perkins, K.S., Rose, P.A., Rousseau, J.P., Orr, B.R., Twining, B.V., and Anderson, S.R., 2002b, Rapid transport of naphthalene sulfonate tracer in the unsaturated and saturated zones near the Big Lost River flood-control areas at the Idaho National Engineering and Environmental Laboratory: Vadose Zone Journal, v. 1, p. 89–101.

Nimmo, J.R., and Mello, K.A., 1991, Centrifugal techniques for measuring saturated hydraulic conductivity: Water Resources Research, v. 27, p. 1263–1269.

Nimmo, J.R., Rubin, J., and Hammermeister, D.P., 1987, Unsaturated flow in a centrifugal field: measurement of hydraulic conductivity and testing of Darcy's law: Water Resources Research, v. 23, p. 124–134.

U.S. Department of Agriculture, 1951, Soil survey manual, p. 208.

van Genuchten, M.Th., 1980, A closed-form equation for predicting the hydraulic conductivity of unsaturated soils: Soil Science Society of America Journal, v. 44, p. 892–898.

van Genuchten, M.Th., Leij, F.J., and Yates, S.R 1991, The RETC Code for quantifying the hydraulic functions of unsaturated soils: U.S. Environmental Protection Agency, EPA/600/2- 91/065, 85 p.

Winfield, K.A., and Nimmo, J.R., 2002, Controlled liquid-volume, *in* Dane, J.H. and Topp, G.C. eds., Methods of soil analysis, Part 4: Physical methods, American Society of Agronomy, Soil Science Society of America, Madison, Wisc., p. 698–703.